Analytical Methods

Reduction of Blood Volume Required to Perform Paper-Based Hematocrit Assays Guided by Device Design

Journal:	*Analytical Methods*
Manuscript ID	AY-ART-01-2019-000010.R1
Article Type:	Paper
Date Submitted by the Author:	14-Mar-2019
Complete List of Authors:	Fernandes, Syrena; Tufts University, Chemistry Baillargeon, Keith; Tufts University, Chemistry Mace, Charles; Tufts University, Chemistry

Reduction of Blood Volume Required to Perform Paper-Based Hematocrit Assays Guided by Device Design

Syrena C. Fernandes, Keith R. Baillargeon, and Charles R. Mace*

Department of Chemistry, Tufts University, Medford, MA 02155

* corresponding author email: charles.mace@tufts.edu

Abstract

Point-of-care diagnostic tests can provide rapid and accurate information about the health of a patient without relying on the expensive equipment found in centralized laboratories. Not only does the development and application of these assays rely on the means of signal transduction, but also the method by which a sample is procured. In order for point-of-care tests to have real clinical utility, they must use sample types and volumes that are relatively easy to obtain (e.g., fingerstick volumes of blood). In this paper, we demonstrate how the design of a paper-based microfluidic device controls the transport of blood within the device and ultimately influences the development of an assay to measure the hematocrit. We show that, with directed design modifications, altering the dimensions of paper-based devices can greatly reduce the volume of blood required to initiate a hematocrit assay (from 50 μL to only 10 μL) without impacting its analytical performance.

Introduction

Blood contains a wealth of information regarding the health status of an individual and is the "gold-standard" sample for the majority of clinical tests. The method used to collect samples of blood (e.g., venipuncture or capillary sampling) and the resulting volume of sample acquired impacts the number and frequency of tests that can be performed. Acquiring samples of blood from a patient intravenously, even with a trained phlebotomist, can be difficult because of the physical pain (i.e., from needle puncture) and emotional distress (e.g., needle phobia) associated with blood draws, and the possible limited accessibility of a vein (e.g., caused by dehydration).[1] Additionally, if frequent monitoring is required, local swelling and vein collapse can limit the availability of blood. These concerns are even more prominent in infants where the amount of blood that can be collected safely at a given time is substantially less than adults and limited vein access is prioritized to administering therapies.[2]

At the point-of-care (POC), fingersticks are the desired method for sample collection because they are less invasive and simpler to procure than venipuncture. To obtain a sample of blood from a finger (or heel for an infant), a lancet is used to puncture the capillary bed and then blood is collected into a container (e.g., capillary tube, microtainer, or dried blood spot card) for storage or transfer.[3,4] Obtaining a reliable fingerstick can be challenging and, instinctively, users may want to combine multiple sticks or "milk" the puncture site. However, these are not acceptable practices and result in unusable samples of blood.[5] Fingersticks and heelsticks generate smaller volumes of blood than venipuncture (μL vs. mL, respectively) but are ideal for when blood must be drawn and tested routinely (e.g., blood glucose) or when only few tests are needed from one sample.[6] Consequently, minimizing the volume of blood required to initiate assays becomes a critical parameter in the design of POC diagnostic assays. For example, glucometers to monitor blood glucose and rapid diagnostic tests for infectious diseases (e.g., malaria) may require as little as 5 μL of sample to perform the assay.[7,8]

Recently, we developed a device to determine the hematocrit, the ratio of packed red blood cell volume to total blood volume, that utilized 50 μL of sample.[9] Our paper-based microfluidic device provides an alternative method to centrifugation, which separates the components of whole blood by density in a capillary tube allowing the volume occupied by packed RBCs to be compared to the total volume of sample as measured using fill length. Our device combined both vertical and lateral wicking pathways to deliver a volume-dependent, distance-based readout for the semi-quantitative identification of hematocrit percentages (i.e., binning high, low or normal percentages) without the aid of an instrument. Our initial investigation into the development of the hematocrit assay in a paper-based microfluidic device included an evaluation of multiple materials and channel designs that promoted the transport of RBCs, impeded the transport of white blood cells (WBCs), and provided resolved distances between hematocrit percentages. In this paper, we expand our understanding on how channel area and geometry can be modified to develop hematocrit devices that accommodate smaller volumes of sample and maintain analytical performance. These second-generation hematocrit devices permit the more economical use of the small volumes of blood that can be generated from a fingerstick and may ultimately allow multiple assays to be performed in parallel on a single device if larger volumes of blood are available.[10,11]

Experimental Section

Materials

We purchased Ahlstrom chromatography paper grades 55 (pore size 15 μm) from Laboratory Sales & Service LLC (Branchburg, NJ). We obtained citric acid monohydrate, 45% w/v D-(+)-glucose and 0.5 M ethylenediaminetetraacetic acid (EDTA) from Sigma-Aldrich. We purchased sodium chloride from Fisher Scientific. We purchased trisodium citric acid dihydrate from Amresco. We purchased Critoseal vinyl plastic putty and SafeCrit plastic microhematocrit tubes from VWR. We acquired Flexmount Select DF051521 (permanent adhesive-double faced

liner) from FLEXcon (Spencer, MA). We purchased Fellowes laminate sheets and food coloring dye from Amazon. We acquired samples of whole blood from Research Blood Components (Brighton, MA).

Methods

Live Subject Statement

We obtained washed human red blood cells (type O+) suspended in Alsever's solution from Innovative Research (Novi, MI). Blood was drawn by the vendor from healthy donors in an FDA-licensed facility. We obtained samples of whole blood from Research Blood Components (Brighton, MA). The vendor follows American Association of Blood Banks guidelines for all donors, which includes IRB approved consent to the use of collected blood for research purposes. All research was approved by the Tufts University Institutional Biosafety Committee.

Designing and preparing devices for the hematocrit assay

The paper-based hematocrit assay uses a device comprising two layers: (i) a top layer that acts as a sample inlet while simultaneously removing the majority of WBCs in the sample by filtration and (ii) a bottom layer containing a funnel-shaped inlet to direct the blood from the top layer to a long lateral channel that serves to semi-quantitatively measure the sample hematocrit based on the overall distance of transported RBCs.[9] We designed the hydrophilic areas of our paper-based microfluidic devices for hematocrit assays using Adobe Illustrator. Using the original hematocrit assay as a basis, we uniformly scaled the features of the design of the original two-layer paper-based device (device **1**) to generate devices that required 35 μL, 25 μL, and 10 μL of blood (devices **2–4**, respectively) to initiate the assay. We did not alter the overall footprint of the device, so the final footprint of the two-layer device (13 mm x 65 mm) remained unchanged. However, for device **4**, we reduced the length of the top layer by 3 mm to a final length of 15 mm in order to have an unobstructed view of the lateral channel on the bottom layer and facilitate the assay readout.

We printed device designs for each layer onto Ahlstrom grade 55 chromatography paper using a Xerox ColorQube 8580 solid ink printer.[12] The printed layers were placed into a 150 ˚C oven for 30 seconds to ensure that the wax melted and permeated the full thickness of the paper. We patterned sheets of double-sided adhesive using a Graphtec Cutting Plotter (CE6000-40) and used Flexmount double-sided adhesive to affix the two layers of the paper-based microfluidic devices. We used sheets of Fellowes laminate to enclose the exposed area of the channel layer to minimize evaporation and to protect the surrounding area and user from potentially hazardous biological materials.

Prior to assembly, we treated the bottom layer with reagents using previously optimized conditions[9] that were modified for the scaled geometries of each device. We prepared solutions of 50 mM NaCl in 18.2 MΩ DI H_2O and 4.5 mM EDTA in 18.2 MΩ DI H_2O. For the original device (i.e., 100% scaling), we added 40 µL of 50 mM NaCl to the lateral channel on the bottom layer and allowed the solution to travel the length of the channel. We then placed the layer in an oven at 65 ˚C for 5 minutes. Next, we added 40 µL of 4.5 mM EDTA and repeated the drying process. We varied the volumes of each solution for alternative designs with reduced hydrophilic areas: device **2** was treated with 30 µL, device **3** was treated with 20 µL, and device **4** was treated with 8 µL.

Preparation of samples of physiologically relevant hematocrit percentages

Samples of washed and packed human red blood cells (RBCs) in Alsever's solution were received at approximately 20% hematocrit, which we determined by centrifugation method. We transferred 20 µL of sample into an untreated microhematocrit tube and sealed one end of the tube with Critoseal. We centrifuged the microhematocrit tube at 800 g for 3 minutes and then scanned the tube with an 8-bit EPSON Perfection V600 PHOTO scanner. We determined the hematocrit of the sample by measuring the ratio of length occupied by the packed RBCs to the total length of sample in the tube in ImageJ.[13] We prepared physiologically relevant hematocrit samples from the RBCs by removing the appropriate amount of volume of Alsever's

solution as previously described.[9] When needed, we diluted samples of RBCs to a lower hematocrit by adding Alsever's solution to the sample. We prepared Alsever's solution using 7.2 mM sodium chloride, 2.7 mM trisodium citric acid dihydrate, 260 μM citric acid monohydrate, and 11.4 mM D-(+)-glucose in 18 MΩ DI H_2O at pH 6.50. After dilution or concentration, we confirmed the hematocrit of each sample using centrifugation. To perform paper-based hematocrit assays with whole blood, we prepared samples in the same manner as described above. However, with whole blood, we used native plasma instead of Alsever's solution as the diluent to obtain lower hematocrit percentages. We centrifuged 2 mL of sample at 800 g for 5 minutes to obtain plasma for dilutions. Samples of whole blood were received in K_2EDTA vacutainers and were used the same day they were drawn from donors.

Performing the hematocrit assay in paper-based devices

We initiated the hematocrit assay by applying a sample to the top layer of the paper-based microfluidic device using a volumetric micropipette. We added 50 μL of sample for the original design, device **1**, 35 μL for device **2**, 25 μL for device **3** and 10 μL for all versions of device **4**. We determined the time for the assay to be completed when the sample no longer travels an appreciable distance in the device. Assays are completed in 30 minutes for device **1**, device **2** and device **3**. However, assays conducted using device **4**, were completed in 10 minutes for all hematocrit percentages. We scanned the devices using the 8-bit EPSON Perfection V600 PHOTO scanner with a resolution of 800 dpi, which was used to convert pixels to inches for measuring the distance traveled by our sample in ImageJ. To obtain the total distance traveled by the sample in our devices, we measured the distance from the top of the circular zone to the leading edge of the sample in the channel. We then subtracted the distance from the top of the circular zone to the entrance of the thin channel allowing the measurement of distance traveled to reflect the distance traveled within the thin channel. A "negative" distance would thus indicate that the sample did not enter the channel, which sometimes occurred with samples of whole blood at high hematocrits. The measurements were then normalized to the

total length of the thin channel for each design so that the performance of the hematocrit assay in each device design can be directly compared to one another (**Figure S1**). We used Prism 7 (GraphPad) to perform linear regression analysis on the concentration curves and to perform statistical analysis on the slopes of the linear fits.

Analyzing the total area of the lateral channel

After we modified the major geometric features of the lateral channel to the final dimensions, we analyzed total area of the irregular shape to enable quantitative comparisons between designs. Device designs were exported from Adobe Illustrator as PNG files. Using ImageJ,[13] we converted each file to an 8-bit, black and white image. We used the line tool to measure the distance of the diameter of the circle. We used the threshold feature to identify the boundaries of the irregular shape of the segmented channel based on greyscale intensities: hydrophilic areas were white, while the patterned hydrophobic areas were black (i.e., from colored wax). We used the wand tool to highlight and select the channel. We then used the measure tool to obtain the total area in mm^2 of the highlighted zone, which enabled direct comparisons in patterned areas between different device designs as “percent area”.

Results and Discussion

Determining relationship between sample volume and channel area

The fluidic pathway assembled in paper-based microfluidic devices directly influences important assay parameters such as assay time, signal intensity, and the volume of sample required to initiate an assay.[14,15,16,17] Because samples can only be transported by capillary action through hydrophilic zones of the device, the total area of the fluidic pathway dictates the fill volume needed to activate and complete an assay. Therefore, increasing or decreasing the hydrophilic area changes the volume needed to fill devices allowing the use of small sample volumes recovered from fingersticks[18] and other sample types (e.g., tears).[19,20] Additionally, defined hydrophilic zones enable functions in paper-based microfluidic devices, such as built in

assay "timers,"[21] distance,[22,23] and text-based readouts[24,25] that can easily be interpreted by a user. These capabilities depend on reproducibly applying specific volumes of sample to the device with the aid of micropipettes or inexpensive, pre-metered capillary tubes. The use of such sample application aids may require training for devices operated by non-experienced users in non-laboratory conditions.

Our investigation into fabricating devices that required smaller volumes of sample to initiate the hematocrit assay began by reducing the total hydrophilic area our original hematocrit device **1**. We uniformly scaled the dimensions of the major geometric features (circle, wide rectangle, thin rectangle) of the original segmented channel design to create devices with reduced channel areas, which would then require smaller volumes of blood to fill the devices and conduct hematocrit assays (**Figure 1A**). For our initial assessment, we maintained the segmented channel design because it was significant to the performance of device **1**. Briefly, we previously observed that the wider, rectangular channel of the segmented design permitted the transport of higher hematocrit percentages into the readout channel, while the thinner, rectangular channel was needed to resolve the distance between different hematocrits. Because the total fill volume of the device is dependent on the unpatterned area, we wanted to quantify the total area of the lateral channel. We determined that the modifications to the original design (device **1**) resulted in an overall change to the unpatterned area of the channel by 82% for device **2**, 58% for device **3**, and 25% for device **4**. These changes correspond to volumes of 35 µL, 25 µL and 10 µL, respectively.

Evaluation of hematocrit assay using smaller channel areas

We examined the influence of reduced channel area and sample volume on assay performance for devices **1–4** using a range of hematocrit samples made from washed and packed RBCs stored in Alsever's solution, a preservative buffer. We have previously demonstrated that RBCs suspended in Alsever's solution and RBCs in whole blood travel through paper differently.[9] While the ultimate paper-based device and hematocrit assay must be

capable of performing measurements using whole blood, the use of washed RBCs offer several advantages over whole blood for performing experiments related to evaluating device design: (i) Washed RBCs are 'purified' samples and contain no other cell types. (ii) Unlike whole blood, which is unstable and whose properties (e.g., hematocrit) change over time,[26] washed RBCs in Alsever's solution have a long shelf-life when refrigerated (ca. weeks).[27] As a result, the experimental conditions surveyed and replicates needed to make conclusions on the relationship between device design and RBC transport are based on fewer variables.

We maintained the same device conditions (i.e., treatment of lateral channel with NaCl and EDTA) and paper with a 15-μm pore size as previously described.[9] However, to directly compare the results of the hematocrit assay between the varying geometries, we normalized the distance traveled by the sample in the thin channel to the total length of the thin channel (i.e., transport on a scale of 0–100% rather than magnitude in mm). Using a physiologically relevant range of hematocrit percentages (62–38%), we observed differences in transport resolution (i.e., slope) between the four devices, with the poorest resolution occurring with device **4** (**Figure 1B**). This is in contrast to the slopes of the assays where only Alsever's solution was added to each new device design; the slopes from all four data sets were determined to not be significantly different ($p=0.558$, **Figure S2**). We attribute the decrease in performance as we decrease the area of the lateral channel to the geometry of the smaller channel areas—predominately the narrowing of the width of the thin channel where the assay readout occurs physically restricting the lateral transport of the RBCs. The effect of a narrow channel width is evident, in particular with device **4** where we observed that the transport distances for the lower hematocrits (<45%) were also severely diminished when compared to the other designs. We hypothesized that the reduced resolution for device **4** may have been caused by: (i) reduced volumes of carrier fluid (e.g., Alsever's solution) present to facilitate RBC transport, and (ii) the narrow width of the thin channel increased RBC crowding at the entrance.

Optimization of hematocrit assay requiring 10 μL sample volume

We chose to optimize the performance of device **4** because we desired a device that required low volumes of blood. Furthermore, the reduced transport distance inherent to the altered lateral channel design of device **4** decreases the assay time to 10 mins, which is three-fold faster than our original hematocrit assay. This trend between assay duration and channel length was expected based on the fundamental process of capillary action in paper (i.e., fluids will wick a certain distance over a specified time period) and is consistent with experimental observations made by our group[28] and others[29,30,31]. When designing alternative versions of device **4**, we strived to maintain a low percent area (<30%) for the channels to preserve the use of 10 µL as our sample volume. We made two notable changes to the channel of device **4**: (i) We first altered the segmented design into a funnel-shape. This change was driven by our hypothesis that the original design accumulated dead volume in the corners of the wide rectangle, and less total volume of blood was therefore available to enter the channel and contribute to the assay. In a volume-dependent assay, this waste could negatively influence assay performance. (ii) We next increased the width of the thin channel. This change was driven by our hypothesis that increasing the amount of porous volume available (via increased channel width) would promote the transport of RBCs by minimizing crowding of cells in a restricted channel (**Figure 2A**).

We evaluated the performance of the alternative designs for device **4** using a range of hematocrits made from of RBCs in Alsever's solution. We observed greater transport distances for the lower hematocrits and consequently, improved transport resolution (**Figure 2B**). Device **4c**, which had both the wider thin channel and funnel-shape, performed comparably to device **1**, the original design despite the difference in sample volume requirements (**Figure 3**). We first evaluated the reproducibility of device **4c** using RBCs in Alsever's solution**.** We applied a sample of RBCs at a 41% hematocrit to twenty devices (**Figure S3**) and determined the coefficient of variation (CV) to be 4.7%. The average distance traveled was 17.1 ± 0.8 mm, which correlated to 85.5% of the total length of the thin channel.

Hematocrit assays using smaller volumes of whole blood

We compared the analytical performance of the hematocrit assay using samples of whole blood for the devices that require 10 µL sample, device **4** and **4c**, to the original device design, device **1**. The optimized device for the assays that require 10 µL of sample volume, device **4c**, performed considerably better than device **4** (**Figure 4**) when we compare the differences in transport resolution between the two data sets. The increase in magnitude of transport resolution for device **4c** indicates that the design adjustments to improve cell transport using samples of RBCs were applicable to samples of whole blood. Additionally, we compared the performance of device **1** to device **4c** and determined that the slopes of these two data sets are not significantly different (p=0.646). We further evaluated the reproducibility of devices **1** and **4c** using samples of whole blood at various hematocrits. We applied each sample of whole blood to five devices and determined the distance (mm), standard error of the mean (mm), and CV (%) for devices **1** and **4c** (**Table 1**). Hematocrits at the outer bounds of our dynamic range (e.g., 60% and 20%) yielded CVs ≤20% indicating high precision in the distance-based readout. While hematocrits in the "normal range" (e.g., 30% and 40%) yielded slightly higher CVs in device **4c**. The average CVs for all measurements in both devices were similar (18% vs. 17% for devices **1** and **4c**, respectively) and comparable to the gauge error we previously calculated for the reference centrifugation method.[26] These results suggest that, with the appropriate modifications to our original hematocrit design, it is possible to reduce the amount of volume required to perform a hematocrit assay in paper-based microfluidic devices and maintain analytical performance.

Conclusions

The successful implementation of POC devices in remote clinics with limited capabilities, in emergency scenarios, or even in homes not only requires the devices to be deployable and easy-to-use but also capable of operating on samples that are relatively easy to attain (e.g.,

urine or blood from a fingerstick). While an important research focus is rightly on the development of the assays used to detect and measure molecular or cellular indicators of health, it is also critical to consider variables related to the sample itself—its method of collection, available volumes, and any required preparation.[32] For samples of blood in particular, these parameters may ultimately dictate whether an assay is suitable for use at the point-of-care. By modifying the design of paper-based devices, we were able to reduce the volume required to conduct a hematocrit assay from 50 μL to only 10 μL. Developing devices that operate with small volumes of blood without sacrificing assay performance would have the dual benefit of using a sample economically (e.g., to enable multiplexing) and potentially reducing the pain associated with conducting a fingerstick.[33,34] Concomitant with this reduction in volume is a substantial decrease in time required to complete the assay: results can be interpreted after only 10 minutes instead of the 30 minutes, which was required by the original hematocrit device due to the long length of the lateral readout channel (20 mm vs. 40 mm).9 While this timeframe is still longer than traditional centrifuge-based methods (ca. 3 minutes),[35] paper-based devices have the benefit of not needing any external equipment or requiring the user to perform any operations aside from adding a sample to the device. Because the hematocrit is a volume-dependent measurement, an accurate deposition of a precise volume of blood is critical to both the performance of the device and also the interpretation of results by a user. However, similar requirements exist for other diagnostic assays that have been designed for use at the point-of-care or limited-resource settings (e.g., malaria,[36] sickle cell disease,[37] and hemoglobin[38]), which suggests that this critical limitation is realistically surmountable using disposable, metered capillaries to dispense accurate volumes of blood.

The reductions in both sample volume and time were enabled by making modifications to two critical aspects of the paper-based microfluidic device: (i) the total unpatterned, hydrophilic area of the device and (ii) the funnel geometry that feeds blood into the readout channel from the sample inlet. The relationship between unpatterned area and sample volume

is clear—larger volumes of sample are required to fill larger areas of unpatterned paper. The latter relationship between channel geometry and assay performance, however, was more nuanced. Not only did we observe that a direct scaling of dimensions resulted in devices with poor analytical performance, but the width of the lateral channel used to transport blood also provided a second constraint that needed to be considered carefully during the design of alternative device geometries. Ultimately, we identified a balance between minimizing dead volume within the funnel and channel width that recovered assay sensitivity and dynamic range for clinically-relevant hematocrits in whole blood. It is clear that further investigations into how the colloidal nature of blood impacts its transport through porous media would greatly support efforts to create fundamental design rules to guide the development of POC assays for hematology.[39,40,41]

Acknowledgements

This work was supported by Tufts University and by a generous gift from Dr. James Kanagy. This material is based upon work supported by the National Science Foundation Graduate Research Fellowship Program under Grant No. (DGE-1325256) that was awarded to S.C.F.

Figure 1. Scaling the device design for paper-based hematocrit assays. (A) Illustrations of alternative device designs created by uniformly scaling the blood transport channel of the original device (device **1**). Each image is labeled with the total area of the lateral channel (i.e., unpatterned paper; in mm^2), which is also expressed as a percent area in comparison to device **1**. As the total area of the lateral channel decreases, less volume (50 μL vs. 10 μL) is required to conduct a hematocrit assay. The dashed lines denote the locations on the device where the readout is measured, which is expressed as a percentage of the total length of the channel (i.e., normalized). (B) Comparison of the normalized distance traveled for a range of hematocrit percentages (62–38%) using a suspension of red blood cells in Alsever's solution for each scaled device design. Each data point is the average of five replicates and the error bars represent the standard error of the mean. Each data set is fit using linear regression to illustrate the relationship between hematocrit and normalized transport distance.

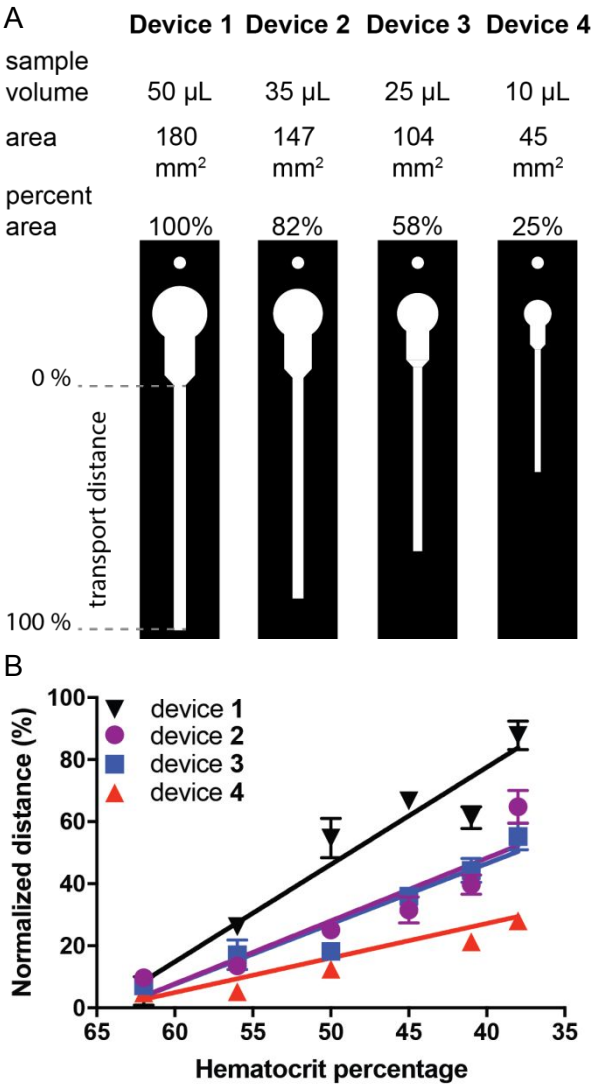
A
Device 1
Device 2
Device 3
Device 4
sample volume
50 µL
35 µL
25 µL
10 µL
area
180 mm²
147 mm²
104 mm²
45 mm²
percent area
100%
82%
58%
25%
0 %
transport distance
100 %
B
Normalized distance (%)
device 1
device 2
device 3
device 4
Hematocrit percentage

Figure 2. Optimization of the channel design for paper-based devices that require only 10 µL of blood to conduct a hematocrit assay. (A) Illustrations of alternative versions of the smallest channel design based around device **4**. Each image is labeled with the total area of the lateral channel (i.e., unpatterned paper), which is also expressed as a percent area in comparison to the original device design (device **1**). (B) Performance of the hematocrit assay using samples of isolated red blood cells in Alsever's solution for a range of hematocrit percentages for each device design. Each data point is the average of five replicates and the error bars represent the standard error of the mean. Each data set is fit using linear regression to illustrate the relationship between hematocrit and normalized transport distance.

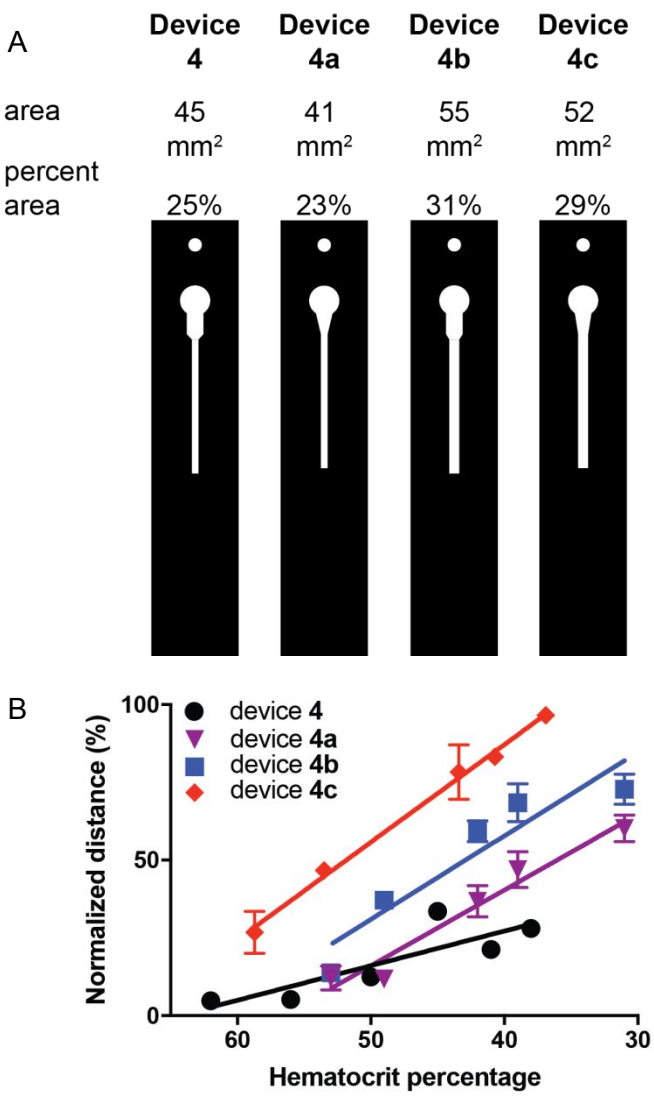

Figure 3. Comparison of paper-based hematocrit assays using the original device design (device **1**, black squares) and the newly optimized lateral channel design (device **4c**, red circles). Assays were performed using 50 μL (for device **1**) and 10 μL (for device **4c**) of red blood cells in Alsever's solution prepared at various hematocrit percentages. Each data point is the average of five replicates and the error bars represent the standard error of the mean. Each data set is fit using a linear regression (device **1**: R^2=0.933, slope=3.133; device **4c**: R^2=0.996, slope=3.135).

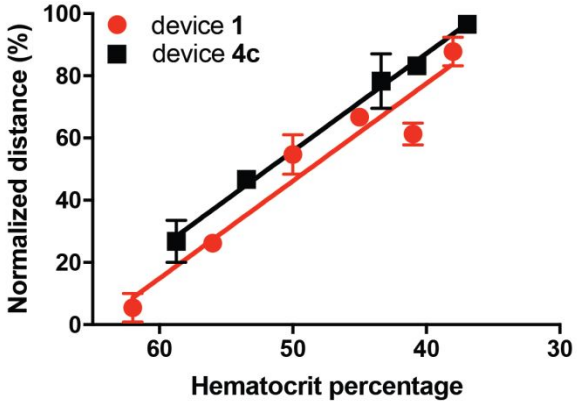

Figure 4. Measurement of the hematocrit of whole blood using different designs of paper-based microfluidic devices. (A) Comparison of the performance of hematocrit assays using device **1** (black), device **4** (blue), and device **4c** (red). Each data point is the mean of five replicates and the error bars represent the standard error of the mean. Each data set is fit using a linear regression (device **1**: R^2=0.938, slope=2.494; device **4c**: R^2=0.929, slope=2.666; device **4**: R^2=0.892, slope=0.6137). (B) Representative images of completed hematocrit assays performed using device **4c**.

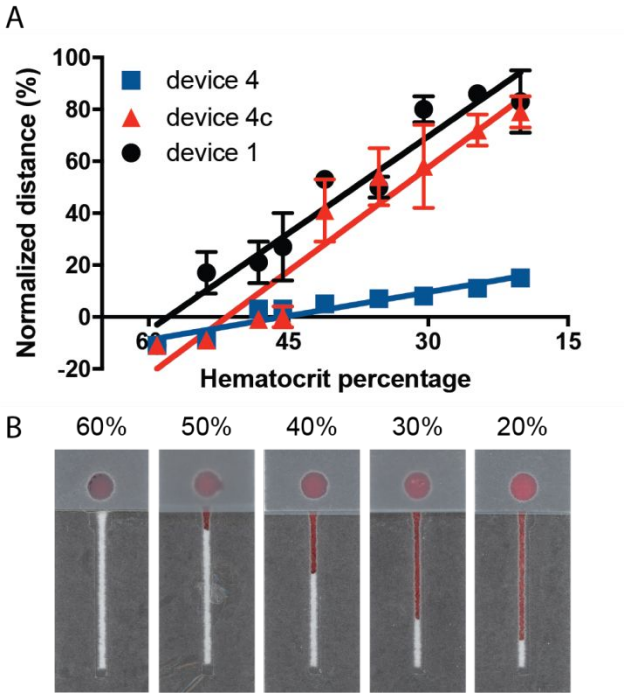

Table 1. Reproducibility of paper-based hematocrit assays performed using devices **1** and **4c**. Samples of whole blood were prepared at various hematocrits and were applied to five devices. The average distance (mm), standard error of the mean (mm), and coefficient of variation (CV) are reported for each hematocrit sample.

	Device **1**			Device **4c**		
Hematocrit	Distance (mm)	SEM (mm)	CV	Distance (mm)	SEM (mm)	CV
59%	-4.4	0.7	16%	-2.2	0.1	6%
54%	7.0	3.2	46%	-1.7	0.3	15%
41%	21.3	1.2	5%	8.3	2.4	29%
31%	32.0	2.1	7%	11.6	3.2	28%
20%	33.3	5.0	15%	15.7	1.2	7%

Table of Contents

We demonstrate device design considerations that enable the scaling of a paper-based microfluidic device to measure the hematocrit of whole blood using only 10 µL of sample.

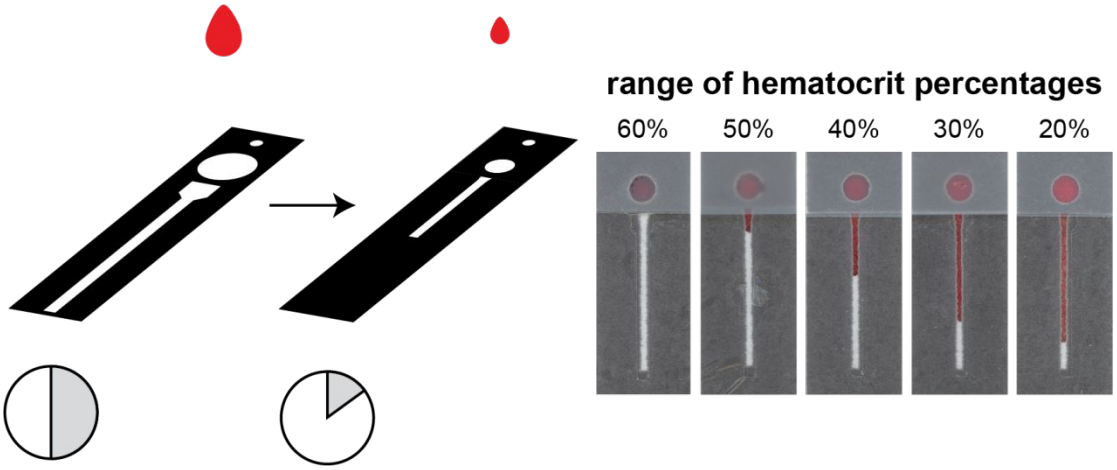

References

1. C. Lalongo and S. Bernardini, *Biochem. Med*., 2016, **26**, 17–33.

2. S. Meites, *Clin. Chem*., 1988, **34**, 1890–1894.

3. P.B. Goldenfarb, F.P. Bowyer, E. Hall and E. Brosious, *Am. J. Clin. Pathol*., 1971, **56**, 35−39.

4. P.A. Demirev, *Anal. Chem*., 2013, **85**, 779–789.

5. M.M. Bond and R.R. Richards-Kortum, *Am. J. Clin. Pathol*., 2015, **144**, 884–894.

6. J.L. Krleza, A. Dorotic, A. Grzunov and M. Maradin, *Biochemia Medica*, 2015, **25**, 335–338.

7. Z. Yared, K. Aljaberi, N. Renouf and J.-F. Yale, *Diabetes Care*, 2005, **28**, 1836–1837.

8. CareStart Malaria Rapid Diagnostic Test, URL: http://www.accessbio.net/eng/products/products01_02.asp (Accessed September 2, 2018.)

9. S.B. Berry, S.C. Fernandes, A. Rajaratnam, N.S. DeChiara and C.R. Mace, *Lab Chip*, 2016, **16**, 3689–3694.

10. R.N. Deraney, C.R. Mace, J.P. Rolland and J.E. Schonhorn, *Anal. Chem*., 2016, **88**, 6161–6165.

11. A.F. Sauer-Budge, S.J. Brookfield, R. Janzen, S. McGray, A. Boardman, H. Wirz, N.R. Pollock, PLoS ONE, 2017, **12**, e0183625.

12. E. Carrilho, A.W. Martinez, G.M. Whitesides, *Anal. Chem.* 2009, **81**, 7091–7095.

13. C.A. Schneider, W.S. Rasband and K.W. Eliceiri, *Nat. Methods*, 2012, **9**, 671−675.

14. E. Fu, T. Liang, P. Spicar-Mihalic, J. Houghtaling, S. Ramachandran and P. Yager, *Anal. Chem.*, 2012, **84**, 4574–4579.

15. G.E. Fridley, H. Le, and P. Yager, *Anal. Chem*., 2014, **86**, 6447–6453.

16. K. Tenda, R. Ota, K. Yamada, T.G. Henares, K. Suzuki and D. Citterio, *Micromachines*, 2016, **7**, 80.

17. G.G. Morbioli, T. Mazzu-Nascimento, L.A. Milan, A.M. Stockton and E. Carrilho, *Anal. Chem*., 2017, **89**, 4786−4792.

18. N.R. Pollock, J.P. Rolland, S. Kuma, P.D. Beattie, S. Jain, F. Noubary, V.L. Wong, R.A. Pohlmann, U.S. Ryan and G.M. Whitesides, *Sci. Transl. Med*. 2012, **4**, 152ra129.

19. K. Yamada, S. Takaki, N. Komuro, K. Suzuki and D. Citterio, *Analyst* 2014, **139**, 1637−1643.

20. K. Yamada, T.G. Henares, K. Suzuki and D. Citterio, *ACS Appl. Mater. Interfaces*, 2015, **7**, 24864–24875.

21. H. Noh and S.T. Phillips, *Anal. Chem*. 2010, **82**, 8071–8078.

22. D.M. Cate, W. Dungchai, J.C. Cunningham, J. Volckens and C.S. Henry, *Lab Chip*, 2013, **13**, 2397–2404.

23. D.M. Cate, S.D. Noblitt, J. Volckens and C.S. Henry, *Lab Chip*, 2015, **15**, 2808–2818.

24. K. Yamada, K. Suzuki and D. Citterio, *ACS Sens*., 2017, **2**, 1247–1254.

25. M. Li, J. Tian, M. Al-Tamimi and W. Shen, *Angew. Chem. Int. Ed.* 2012, **51**, 5497–5501.

26. L.P. Murray, K.R. Baillargeon, J.R. Bricknell and C.R. Mace, *Anal. Methods* 2019, **11**, 930–935.

27. Y.V. Kucherenko and I, Bernhardt, *Cell. Physiol. Biochem.* 2015, **35**, 2055–2068.

28. J.E**.** Schonhorn, S.C. Fernandes, A. Rajaratnam, R.N. Deraney, J.P. Rolland and C.R. Mace, *Lab Chip* 2014, **14**, 4653–4658.

29. S. Jahanshahi-Anbuhi, P. Chavan, C. Sicard, V. Leung, S.M.Z. Hossain, R. Pelton, J.D. Brennan and C.D.M. Filipe, *Lab Chip*, 2012, **12**, 5079–5085.

30. E. Fu, T. Liang, P. Spicar-Mihalic, J. Houghtaling, S. Ramachandran and P. Yager, *Anal. Chem.*, 2012, **84**, 4574–4579.

31. M. Cummins, R. Chinthapatla, F.S. Ligler and G.M. Walker, *Anal. Chem.*, 2017, **89**, 4377−4381.

32. T.M. Blicharz, P. Gong, B.M. Bunner, L.L. Chu, K.M. Leonard, J.A. Wakefield, R.E. Williams, M. Dadgar, C.A. Tagliabue, R. El Khaja, S.L. Marlin, R. Haghgooie, S.P. Davis, D.E. Chickering and H. Bernstein, *Nat. Biomed. Eng*., 2018, **2**, 151–157.

33. H. Fruhstorfer, G. Schmelzeisen-Redeker and T. Weiss, *Eur. J. Pain.*, 1999, *3*, 283–286.

34. L. Heinemann and D. Boecker, *J. Diabetes Sci. Technol.*, 2011, **5**, 966–981.

35. R.A.W. Scott, G.L. Hortin, T.R. Wilhite, S.B. Miller, C.H. Smith and M. Landt, *Clin. Chem*., 1995, **41**, 306–311.

36. Abbot Rapid Diagnostics. BinaxNOW Malaria. https://www.alere.com/en/home/product-details/binaxnow-malaria.html (accessed 1 Mar 2019)

37. A.A. Kumar, C. Chunda-Liyoka, J.W. Hennek, H. Mantina, S.Y. Lee, M.R. Patton, P. Sambo, S. Sinyangwe, C. Kankasa, C. Chintu, C. Brugnara, T.P. Stossel and G.M. Whitesides, *PLoS One* 2014 **9**, e114540.

38. E.A. Tyburski, S.E. Gillespie, W.A. Stoy, R.G. Mannino, A.J. Weiss, A.F. Siu, R.H. Bulloch, K. Thota, A. Cardenas, W. Session, H.J. Khoury, S. O'Connor, S.T. Bunting, J. Boudreaux, C.R. Forest, M. Gaddh, T. Leong, L.A. Lyon and W.A. Lam, *J. Clin. Investig.* 2014, **124**, 4387–4394.

39. M.S. Khan, G. Thouas, W. Shen, G. Whyte and G. Garnier, *Anal. Chem*. 2010, **82**, 4158–4164.

40. L. Li, X. Huang, W. Liu and W. Shen, *ACS Appl. Mater. Interfaces*, 2014, **6**, 21624–21631.

41. S.C. Fernandes, J.A. Walz, D.J. Wilson, J.C. Brooks and C.R. Mace, *Anal. Chem.*, 2017, **89**, 5654–5664.